Research Article

Design of an Adaptive Neural Network Controller for Effective Position Control of Linear Pneumatic Actuators

Osama. A. Montasser[A*] and B. A. El-Sayed[B]

[A]Mechanical Power Engineering, Ain Shams University, Cairo, Egypt, on leave to join the British University in Egypt, BUE

[B]Sakr Facroty, The Arab Organization for Industrialization (AOI), Cairo, Egypt

Abstract

The main target of this work is to design an appropriate position controller for a pneumatic system using artificial neural networks. The rod position of a double acting pneumatic cylinder, controlled by proportional linear valves, was chosen as the present control system. A mathematical dynamic model for the pneumatic system was derived. The model shows, as it is expected, that the pneumatic system is of highly nonlinear features. This is due to cylinder-piston mechanical friction, the compressibility feature of air, and nonlinear characteristics of the flow through a valve orifice of variable area. The model shows, as well, that pneumatic system is of time varying characteristics. A Proposed Neural Network Controller, PNNC, is designed and implemented. The PNNC is a rule-based controller, where both the slope and amplitude of the activation function of each neuron is adapted to enhance the control system performance. A considerable improvement of the system response for different input conditions is achieved by applying the PNNC on the present control system. The robustness and effectiveness of the proposed controller were verified through computer simulations using MATLAB package and SIMULINK toolbox. A comparison with the Conventional Neural Network Controller, CNNC and the typical PID controller, assured that the present PNNC is robust and more efficient in terms of both the system stability and speed of response.

Keywords: Accurate Position Control, Adaptive Learning Algorithm, Neural Network Controllers, Pneumatic Actuators, Sigmoid Activation Function.

1. Introduction

Hydraulic actuators are relatively easy to be positional controlled than the pneumatic actuators. This is due to the high nonlinearity associated with pneumatic media flow. A self-tuning fuzzy PID controller was successfully developed and applied to an electro-hydraulic actuator by (N. Ishak *et al*, 212). The proposed controller offers promising capabilities to guarantee the position tracking accuracy of their hydraulic system.

However, Pneumatic actuators are now a recognized alternative technology to other hydraulic and electric counterparts in areas of high speed, medium power applications (J. Moore and C. Wong, 2000). Pneumatic systems are capable of providing suitable power output at relatively low cost, in addition they are clean, of light weight and can be easily serviced. Pneumatic actuation has been mainly used in the form of logic control systems.

Many applications in industry use pneumatic power in open loop control systems where the strokes of the moving parts are usually fixed using mechanical stops. However, many other applications require the position control of pneumatic cylinders such as, robots, gating systems and

CNC machines. (N. Tillet *et al*, 1997) provided that pneumatic systems have been limited to a simple end-stop application because of the difficulty of providing proportional control of the rod position. This difficulty stems from the nonlinear nature of air as power transmission medium and non-linearity associated with pneumatic components (M. Shih and M. Ma, 1998).

(Verseveld and Bone, 1997) proposed position controlled pneumatic actuator. This pneumatic system consists of a double acting cylinder, with low friction option, connected to a horizontal linear slide. A pneumatic brake mechanism is incorporated within the linear slide to lock the actuator firmly in its position once the desired steady state accuracy is achieved. Two standard three-way solenoid valves were used. The valves were actuated using a Pulse Width Modulation algorithm, PWM. A PID controller with added friction compensation and position feed-forward is successfully implemented. As it is well known, PID controllers are widely used for process control because of their good performance. However, it is very difficult to self tuning the control parameters of these controllers.

(K. Fujiwara and Y. Ishida, 1995) described a method of using neural networks to self-tuning the PID controllers for pneumatic cylinders. They show simulation and

---

*Corresponding author: **Osama. A. Montasser**

experimental results to demonstrate the effectiveness of their model. (M. Shih and M. Ma, 1998) have proposed the applying of a fuzzy control technology to control the position of a pneumatic cylinder. In their work, a modified differential PWM control method was applied.

There are numerous works applied artificial intelligence in the control applications but few of them are used in pneumatic control systems. (X. Cui and K. Shin, 1992) used an Artificial Neural Network Controller, ANNC, to control the middle-point temperature in a thermal power plant. The ANNC was designed to deal with the nonlinearity due to negative effects of long response delays, saturation conditions and process noise. The controller consists of four-layer, with two hidden layers, perceptrons. Their work introduced a simple algorithm based on the Back-Propagation, BP, for a class of nonlinear systems, typified by process control applications. The proposed NN controller is trained using the system's output errors directly, with little a priori knowledge of the controlled plant.

(M. Abdelhameed, 1999) introduced an adaptive neural network controller for tracking a robot of n-degree-of-freedom. The learning algorithm is based on the adaptive updating of the weights of the network to minimizing the quadrant tracking error and its derivative of each robot arm. (G. Geng and G. Geary,1997) proposed a method which uses neural networks together with recursive least square algorithm to model nonlinear processes. (G. Cembrano *et al, 1997*) described the use of Cerebellar Model Articulation Controller (CMAC) networks for the adaptive dynamic control of an orange harvesting pneumatic robot. A neural-network model was preferred since it provided better approximation capabilities.

Finally, it is noticed that the application of conventional control methods on position control of pneumatic systems have some restrictions. Furthermore, there are relatively few works related to the application of artificial neural network controllers in the field of pneumatic actuation systems. It therefore, the main issue considered in the present work is to design an appropriate position control system for a pneumatic actuator using artificial neural networks.
The Artificial Neural Network Controller, ANNC was chosen to position control the piston movement of the present pneumatic system. This is decided to get the benefits of its intelligence and learning capability needed to cope with the higher inflexibility and nonlinearity of the pneumatic systems. A rule based NN controller is proposed, tested and found to successfully achieve a good tracking control performance and is robust to sever changes in the applied load as well.

The present paper is organized as follows. In the following section, mathematical and state space models of the present pneumatic system are derived. An introduction to the artificial neural network based controllers is reviewed afterward. In the next section, the Conventional on-line self learning based Neural Network Controller, CNNC, is introduced. The computational steps used to build a CNNC are listed in subsequent section. A rule based neural network controller is proposed and designed in the following section, PNNC. Results of the present

CNN and PNN controllers are consequently discussed. The conclusions of this study are summarized in the last section.

2. Modeling of the present pneumatic system

In this section a state space model of the present pneumatic system to be positional controlled is derived. Description of the system is presented and the mathematical model of each of its components is derived.

2.1. Pneumatic system description
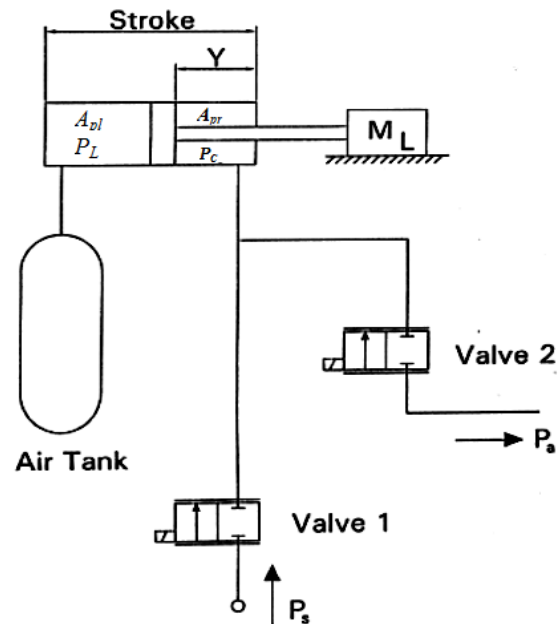
Fig.1 Layout of the present pneumatic system

The present pneumatic system is shown in Figure 1. It consists of a double acting cylinder, linear pneumatic actuator, controlled with two proportional valves, v_1 and v_2, and carrying an external load M_l. Air is discharged from a pressurized air supply to the right hand side of the cylinder through valve1, v_1. The air is discharged from the cylinder to the atmosphere through valve2, v_2.

The pressure at the left hand side of the cylinder is held constant by attaching it with a large accumulator, air pressure in which, P_l, is 2.9 bar. The function of the accumulator is to maintain a reasonable difference of air pressure between right and left sides of the cylinder. This reduces the nonlinearity associated with large pressure difference between both sides of the cylinder. The value of the supply pressure, P_s is fixed at six bar.

When v_1 is opened and v_2 is closed, the air flows through v_1 to the right side of the cylinder, which is initially at force balance state, to increase its pressure, P_c. As P_c increases, the piston of the cylinder moves to the left to the desired position, y_{ref}. v_1 is kept opened, as the position of the piston $y(t)$ is less than the desired piston position y_{ref}. When the piston position $y(t)$ exceeds the desired piston position, y_{ref}, v_1 is closed and valve v_2 is opened to reverse the direction of the piston motion to the right. The air at the right side of the cylinder discharges to

the atmosphere and P_c thus decreases. This lets the piston moves to the desired position at the right side and when reached, the valve v_2 is closed.

2.2. Mathematical modeling

In order to derive the governing equation for the motion of the cylinder piston, the momentum equation is considered as follows:

$$M_l \ddot{y} = P_c A_{pr} - P_l A_{pl} - f_c \dot{y} \tag{1}$$

Where: P_c, P_l are the air pressure at the cylinder right and left side respectively and A_{pr} and A_{pl} are the cross sectional areas of right and left sides of the cylinder respectively, f_c is the viscous damping coefficient, $\dot{y}$ and $\ddot{y}$ are velocity and acceleration of the piston rod and M_l is the equivalent mass of piston head and the load.

The energy equation is applied to obtain a mathematical model for pressure dynamics of the air in the cylinder. Variation in air pressure at the cylinder left side, P_l, is ignored since it is considered constant due to the accumulator effect. Considering the right side of the pneumatic cylinder as a thermodynamic control volume, the governing equation for air pressure P_c is obtained by applying the energy equation as follows:

$$\dot{Q} - P_c \frac{dV_c}{dt} = \left(\dot{m}_2 C_p T_c - \dot{m}_1 C_p T_s \right) + \frac{d(m_c u)}{dt} \tag{2}$$

Where: $\dot{m}_1$ and $\dot{m}_2$ are the air mass flow rates through valves v_1 and v_2 respectively, $\dot{Q}$ is the rate of heat transfer across the cylinder wall, P_c, V_c, m_c and u are pressure, volume, mass and specific internal energy of air at the cylinder right side, $P_c \, dV_c/dt$ is the rate at which work is done on the moving piston, T_s is the supply air temperature and T_c is the air temperature at the cylinder right side, $C_p \left(\dot{m}_2 T_c - \dot{m}_1 T_s \right)$ is the enthalpy difference through the control volume boundaries and $d(Mu)/dt$ is the rate of change of internal energy of the control volume.

Since the mass transfer through the system is much faster than the heat exchange through the system boundary, so, $\dot{Q}$ can be neglected. It was thus reasonably assumed that the system undergoes an adiabatic process. Applying thermodynamics relations for ideal gases, equation (2) is reduced to:

$$\frac{dP_c}{dt} = -\frac{\gamma P_c}{V_c} \cdot \frac{dV_c}{dt} + \frac{\gamma R}{V_c} \left(T_s \dot{m}_1 - T_c \dot{m}_2 \right) \tag{3}$$

Where: γ is specific heat ratio, R is the air gas constant.

While opening valve v_1, the status of air mass flow rate through it, $\dot{m}_1$, changes from moment to moment. It may be directed to inter the pneumatic cylinder, inflow ($\vec{m}_1$), or may directed to leave it, outflow ($\vec{m}_1$). This is due to the high dynamics of air pressure at the right side, P_c, due to which, it may take a lower or higher value than that of

the supply pressure, P_s. Outflow, $\vec{m}_1$, should take a negative sign when it is substituted in energy equation (3). On contrary, the air mass flow rate through valve v_2, $\dot{m}_2$ is always directed to the atmosphere, since P_c never be lower the atmosphere pressure P_a. Relations for $\dot{m}_1$ and $\dot{m}_2$ are concluded as follows:

$$\dot{m}_1 = A_{v1} \, \rho_{v2} \, c_{v1} \, Cd_{v1} \tag{4}$$

$$\dot{m}_2 = A_{v2} \, \rho_{v2} \, c_{v2} \, Cd_{v2} \tag{5}$$

Where: c and ρ is the air velocity and density at the valve orifice, A is the partially opened valve orifice area, A varies from 0% to 100% of the orifice area, and C_d is the valve discharge coefficient. Subscripts v_1 or v_2 refers to the valve number.

Relations for the air density and velocity, ρ and c, through both proportional valves are obtained by applying the continuity equation and the thermodynamic relations for ideal gases as follows:

Proportional valve 1

Two possible conditions for the reduced pressure ratio through the valve, P_R, are considered, namely the subsonic condition for $P_R > 0.528$ and supersonic condition for $P_R \leq 0.528$. Relations for the two conditions are shown as follows:

a) Subsonic condition
a-1) Inflow condition, $P_c < P_s$, $P_R = P_c / P_s) > 0.528$:

$$\rho_{v1} = \frac{P_c}{R \, T_s \, (P_R)^{\gamma-1/\gamma}} \tag{6}$$

$$c_{v1} = \frac{1}{\sqrt{1 - (\rho_{v1} A_{v1} / \rho_s A_s)^2}} \sqrt{\frac{2 \, \gamma \, R}{(\gamma - 1)} T_s \left[1 - (P_R)^{\gamma-1/\gamma} \right]} \tag{7}$$

a-2) Outflow condition, $P_c > P_s$, $(P_R = P_s / P_c) > 0.528$:

$$\rho_{v1} = \frac{P_s}{R \, T_c \, (P_R)^{\gamma-1/\gamma}} \tag{8}$$

$$c_{v1} = \frac{-1}{\sqrt{1 - (\rho_{v1} A_{v1} / \rho_c A_c)^2}} \sqrt{\frac{2 \, \gamma \, R}{(\gamma - 1)} T_c \left[1 - (P_R)^{\gamma-1/\gamma} \right]} \tag{9}$$

where: ρ_s is the density of supplied air and A_s and A_c are the cross sectional areas of the connections of air supply and the cylinder with the valve v_1 respectively.

b) Supersonic condition
For inflow condition, supersonic flow is possible and the air density relations are derived as follows:
b-1) Inflow condition, $P_c < P_s$, $P_R = P_c / P_s \leq 0.528$:

$$\rho_{v1} = \frac{0.528 \, P_s}{\frac{2}{\gamma+1} \, R \, T_s} \tag{10}$$

$$c_{v1} = \sqrt{\frac{2\gamma}{\gamma+1} R T_s} \tag{11}$$

b-2) Outflow condition, Pc > Ps:

Outflow of air from the right side of the pneumatic cylinder to the air supply is always subsonic and cannot be supersonic since P_s / P_c never be possibly less than or equal 0.528.

Proportional valve 2

Since $P_c > P_a$ *in all working conditions*, flow of air from the cylinder to the atmosphere through valve2 is always outflow.

a) Subsonic condition, $P_c / P_a > 0.528$:

$$\rho_{v2} = \frac{P_a}{R T_c (P_R)^{\gamma-1/\gamma}} \tag{12}$$

$$c_{v2} = \frac{1}{\sqrt{1-(\rho_{v1}A_{v1}/\rho_c A_c)^2}} \sqrt{\frac{2\gamma R}{(\gamma-1)} T_c \left[1-(P_R)^{\gamma-1/\gamma}\right]} \tag{13}$$

b) Supersonic condition $P_c / P_a \leq 0.528$:

$$\rho_{v2} = \frac{0.528 P_c}{\frac{2}{\gamma+1} R T_c} \tag{14}$$

$$c_{v2} = \sqrt{\frac{2\gamma}{\gamma+1} R T_c} \tag{15}$$

Where: P_a is the atmosphere pressure.

2.3 State space model

The state space model of the pneumatic system could be derived as follows:
Variables x_1, x_2, x_3 are defined as:

$$x_1 = y, \quad x_2 = \dot{x}_1 = \dot{y}, \quad x_3 = P_c \tag{16}$$

From equations 1, 3 and 16, the following relations are obtained.

$$\dot{x}_2 = \ddot{y} = a_1 x_3 + a_2 + a_3 x_2 \tag{17}$$

$$\dot{x}_3 = \dot{P}_c = a_4 \frac{x_2 x_3}{x_1} + a_5 \frac{1}{x_1} \tag{18}$$

Using the previous derived relations 1 to 15, a_1 to a_5 are calculated as follows:

$$a_1 = \frac{A_{pr}}{M_l} \tag{19}$$

$$a_2 = \frac{-P_l A_{pl}}{M_l} \tag{20}$$

$$a_3 = \frac{-f_c}{M_l} \tag{21}$$

$$a_4 = -\gamma \tag{22}$$

$$a_5 = \frac{\gamma R (T_s \dot{m}_1 - T_c \dot{m}_2)}{A_{pr}} \tag{23}$$

The model, derived above, shows that dramatic changes always occur in the density of air in pneumatic systems. This is due to the high compressibility essential feature of all gases.

3. Artificial neural network based controllers

A great attention has been devoted, in recent years, to the artificial multilayer neural networks, ANNs, which have proved to be extremely successful in pattern recognition and control problems. The main feature of the ANNs is their capability of dealing with nonlinear continuous functions. That is why their applications for controlling complex nonlinear systems have become an essential matter. In the present work, an ANN controller is proposed to be used in positional control of the present pneumatic system.

Fig.2, below, shows the architecture of an artificial neural network of one hidden layer. It consists of three consecutive layers, namely, the input layer, of n dimensions, the neural network hidden layer, of N neurons, and the output layer, of m dimensions. Each of the input and the output vectors is connected with each neuron of the hidden layer through a synaptic weight, which is a real fraction number and is calculated according to an activation function. We, therefore, have two weight matrices, $n \times N$ dimensional matrix for input-neural network layers connections and $N \times m$ dimensional matrix for neural network-output layers connections.

The neurons are connected according to layered feed-forward neural networks method, where a layer of neurons receives input only from neurons of the previous layers.

Various methods could be used to update the weights of the neural network layer, what is so called training the ANN, so that for a certain input to the input layer, we can get the desired output from the output layer. One way is to set the weights explicitly using prior knowledge of the system under consideration, open loop control.

The learning categories are classified into two distinct types, namely the supervised learning and unsupervised learning. In supervised learning, associative learning type, the network, which is called self-supervised, is trained by providing it with inputs and the matching outputs patterns.
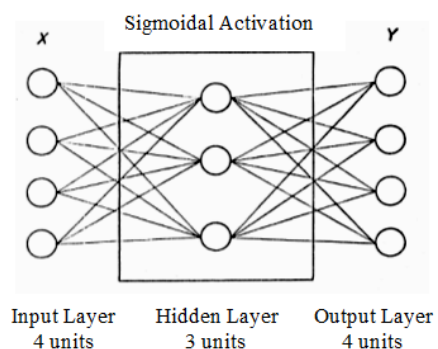
Fig.2 Architecture of an artificial neural network of one hidden layer

Classic applications of ANN control systems are of supervised learning, open loop type. Reasonable accuracy of open loop control using ANN controllers is attained for a certain specified initial-desired output error $e_{initial}$ value. This is achieved through pre-learning the controller for the specified value of $e_{initial}$ to get control actions fairly fitting the inputs to the controller.

Another way is to train the ANN by using a teaching pattern and letting the network sets its weights ON LINE, unsupervised learning. This is carried out according to some predefined learning rules and an error performance index minimization algorithm.

In the unsupervised learning, self-organizing type, the network is trained to respond to clusters of input patterns. Unlike the supervised learning pattern, there is no a priori categories set, according to which the input-output patterns are to be classified, rather, the system should develop its own representation of the input-output relationships.

4. The conventional on line self learning based NN controller, CNNC

Recently, the ANN have been used to control many industrial plants. The online learning by continuous mapping between the inputs and output factors of the controller enables the use of ANN controllers in feed-back control systems. A multilayer perceptron structure with back propagation, BP, learning algorithm is one of the most effective online learning algorithms. It can be used to approximate any continuous function mapping with any desired accuracy. For control purposes, the ANN based controller utilizes the actual system input error to synthesize the control action.

Since, in control systems, it is practically to measure the output from the plant, the controlled variable $y(t)$, rather than the output from the NN controller. It is therefore, the NN based controllers utilize the error in the controlled variable, the deviation between the desired and the actual output, $e(t) = y_{ref} - y(t)$, to synthesize the control action. The error in plant output, $e(t)$, is used also in training the NNC or in other words in updating the weights of the neural network layers.

When designing the NN control system, the major obstacle is to train the NNC using the error in the system-output, $e(t) = y_{ref} - y(t)$, rather than the unknown network-output's output. (X. Cui and K. Shin, 1992) presented a solution for this problem for conventional neural network based controllers CNNC. (X. Cui and K. Shin, 1992), adopted the basic principle of multilayer perceptrons with BP to update the weights of each perceptron. Their formulas for updating the thresholds and the weights from the input to the output layers are utilized in this work to build a conventional neural network position controller CNNC.

The piston rod position, $y(t)$, of the present pneumatic system, shown in Figure 1 above, is controlled using a NN based controller. A block diagram for the present position control system is presented in Figure 3. A neural network controller, NNC, is cascaded with the pneumatic controlled system. The NNC output, control action $\mu(t)$, is

used to modify the opening ratio, k, of the valves, v_1 and v_2, to achieve the desired controlled variable, y_{ref}.
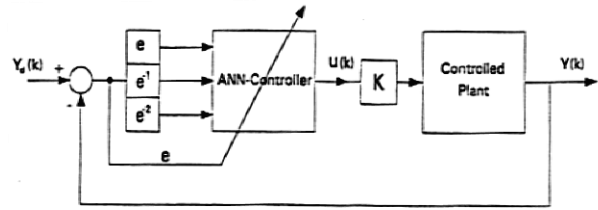
Fig.3 A block diagram for the present position control system

Figure 4 shows the basic structure of the present artificial neural network. The choice of the ANN's inputs should reflect the desired and actual status of the controlled variable. Therefore, the inputs of the ANN controller is usually the system's tracking errors at the current time and at two preceding sampling time intervals, Δt, $e(t)$, $e(t - \Delta t)$, $e(t - 2\Delta t)$. Inputs are selected to consider the history of the rate of change of error signal, $e(t)$, to simulate the integral action in the conventional PID controller. Where Δt is the sampling time interval used in numerical calculations. Δt was selected to be as small as possible to overcome the numerical instability.
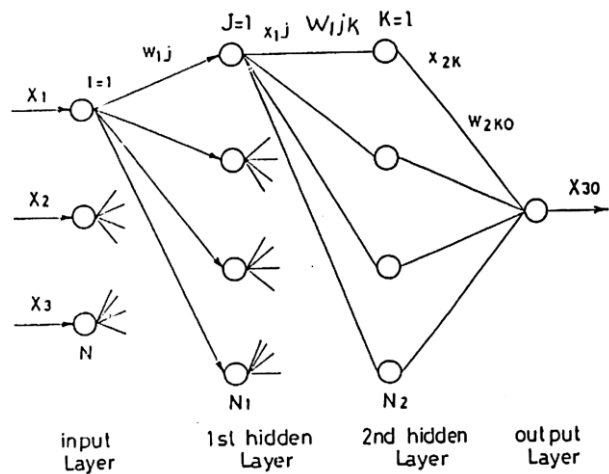
Fig.4 Basic structure of the present artificial neural network

The number of the hidden layers depends on the controlled plant under consideration, and is selected to be two here in this work. The symbols used in Figure 4 are defined as; X: for inputs, $I=1 \rightarrow N$ for input layer, $N=3$ in this work, $J=1 \rightarrow N_1$ for the 1st hidden layer neurons, $K=1 \rightarrow N_2$ for the 2nd hidden layer neurons, N_1 and N_2 are chosen to be 4 in this work, and subscripts *1 , 2* and *3* represent *1st* and *2nd* hidden layers and the output layer respectively. We have only one output from the present NNC, $O = 1$.

5. Computational steps of the CNNC

Computations of the present NN controller, presented in Figure 4, are summarized in this section. The on line self learned CNNC of (X. Cui and K. Shin, 1992) are used here as a conventional position NN controller. Their

formulas for updating the thresholds and the weights from the input to the output layers are utilized in this work.

The activation function considered for each neuron is of the sigmoid type. The sigmoid activation function has the form:

$$x(t) = \frac{1}{1 + e^{-\beta(O+\theta)}} \quad (24)$$

Where: $x(t)$ is the output of a neuron, $O(t)$ is its input, the summation of the outputs of previous layer's neurons multiplied by the corresponding weight factors, $\theta(t)$ is a threshold value, and β is a slope parameter fixed at unity value for the present CNNC, $\beta = 1$. Weight factors, $W(t)$, and thresholds, $\theta(t)$, are initially defined and updated as described below.

A satisfactory control results could not be attained before selecting the optimum values of the initial values of all the weight factors, $W_{initials}$, thresholds, $\theta_{initials}$, learning rates, $\delta_{initials}$, and gain factors, $\eta_{initials}$. Learning rates and gain factors are used to update the weight factors and the thresholds.

The selection of these parameters is very tough and takes a very long time because it depends on trial and error concept. To simplify the process all members of each of the above mentioned parameters are given same initial value. The optimum initial value of any of the parameters is obtained as follows;

As the values of the other parameters are kept constant, the value of the parameters under consideration is changed and at each of its values control performance measures are checked. Performance measures are considered as the settling time, the steady state error, and the root mean square of the error. The value of the parameters under consideration which gives the best combination of the three performance measures is chosen as the optimum initial value of the parameters taken into consideration. The same procedure is repeated for all the other parameters to get, at last, their optimum initial values.

It is worth noting that there is a narrow range of initial values for each of the NNC parameters out of which the control system is unstable. That is why it is very important to carry out the above mentioned selection process not only to get optimum control performance but also to avoid system instability.

The CNNC is trained to achieve a certain control condition, $e_{initial} = y_{ref} - y_{initial}$. Computational steps are carried out according to (X. Cui and K. Shin, 1992) as listed in what follows:

1- For a certain specified $e_{initial}$ and $\beta = 1$, the initial values, $W_{initials}$, $\theta_{initials}$, $\delta_{initials}$, and $\eta_{initials}$ are selected as mentioned above.
2- The outputs of the 1st HIDDEN layer are computed at the current calculation step *(t=0)*.
3- The outputs of the 2^{n} HIDDEN layer are computed at *(t=0)*.
4- The output from output layer, control action, is computed at *(t=0)*.
5- Weights from the 2nd HIDDEN to OUTPUT layers are updated for the next calculation step $(t = t + \Delta t)$.
6- Weights from the 1st HIDDEN to 2nd HIDDEN layers are updated for $(t + \Delta t)$.

7- Weights from the INPUT to 1st HIDDEN layers are updated for $(t + \Delta t)$.
8- The thresholds are updated for $(t + \Delta t)$.
9- Steps from 2 to 8 are repeated for the next calculation step $(t = t + \Delta t)$.

The conventional NN controller was found to be a single point controller and should be set up for each different $e_{initial}$ value and for each piston movement direction. It is therefore it can't be used for tracking position control. A most smart controller was proposed by this study, so that a wide range of initial error values can be efficiently controlled. The Proposed NNC, PNNC, was checked for tracking control in both piston movement directions and found to be successful. The PNNC is presented in the next section.

6. The proposed rule based neural network controller, PNNC

The PNNC is proposed in this study to cover a wide range of control points in both piston movement directions. The same structure, shown in Figure 4, for the CNNC is used.

The slope parameter, β, of the sigmoid activation function, Equation 24, is fixed at unity value with the present CNNC, $\beta = 1$. The slope value affects the degree of nonlinearity of the sigmoid function and thus affects the updating of the NNC parameters. It was found that when the β value is changed the optimum $e_{initial}$ of the CNNC is changed than that at which the optimum initial values of its parameters are selected. So the proposed rule based NN controller, PNNC, was constructed to achieve a successful tracking control as follows:

1- For forward piston movement and a unity slope parameter, $\beta = 1$, a certain initial error, $e_{initial} = y_{ref} - y_{initial}$, is defined and for which, the optimum initial values of the controller parameters are selected as described in section 5.
2- Keeping the optimum initial values unchanged, the value of the initial error, $e_{initial}$, is changed. At each value of the initial error, the value of the slope parameter, β, is changed to meet the best combination of the control performance measures, namely, the settling time, the steady state error and the root mean square of the error value. This is carried out utilizing the trial and error technique.
3- A fairly good curve fitting, correlation factor is almost equal to 1, is concluded for the optimum $(\beta - e_{initial})$ data for the forward piston movement. The curve fitting is resulted in a polynomial form as:

$$\beta = \sum_{i=0}^{s} a_i \; e_{initial}^{i} \text{ , Where } a_i \text{ are constants and } s \text{ is the number}$$

of the polynomial terms.

4- Steps from 1 to 4 is repeated but for the piston backward movement. So that two $(\beta - e_{initial})$ relations are obtained, one for each piston movement's direction. Having the relations the most suitable value of the slope parameter, is calculated at each initial error value and for any piston movement direction, and thus satisfactory control results is achieved.

7. Results of the present control system

The model of the pneumatic controlled plant is built and all the simulation tests are carried out using MATLAB package and SIMULINK toolbox.

7.1. Results of the CNNC

Typical results of the CNNC are shown in Figures 5 and 6. The figures present the control system response with the conventional NN controller. Figure 5 shows the response when the initial error, $e_{initial} = y_{ref} - y_{initial}$, has a value of 4 cm for forward piston movement. This value is the value at which the optimum values of the controller's parameters were determined and mentioned in section 5 above. It is therefore, the system shows satisfactory results as Figure 5 illustrates.
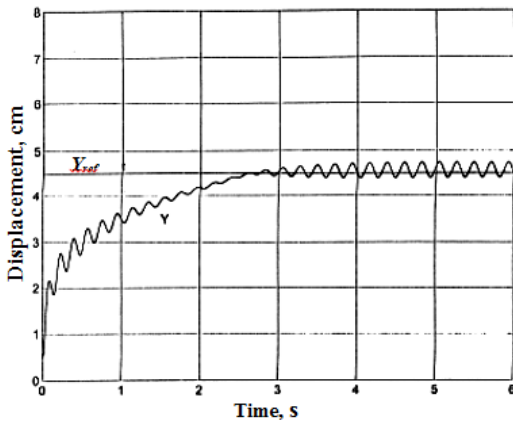
Fig.5 Control system response with CNNC set up for $e_{initial} = 4$ cm

Figure 6 shows different results as the system failed to reach the reference position. The reason is that the initial error is changed to 5.5 cm, the value that is different from the value at which the NN controller's parameters were determined.
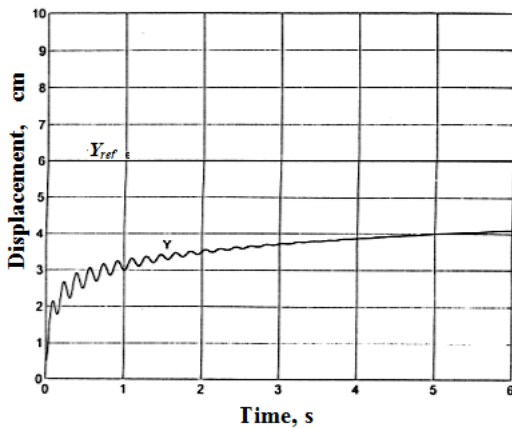
Fig.6 CNNC set up for $e_{initial} = 4$ cm failed to cover $e_{initial} = 5.5$ cm

The CNNC was tested for backward piston movement and found to be also successful for single control point. Of course for the same $e_{initial}$ absolute value each of the

forward and backward position control needs a different initial NN parameters selection. A typical result for the piston backward movement position control is shown in Figure 7.
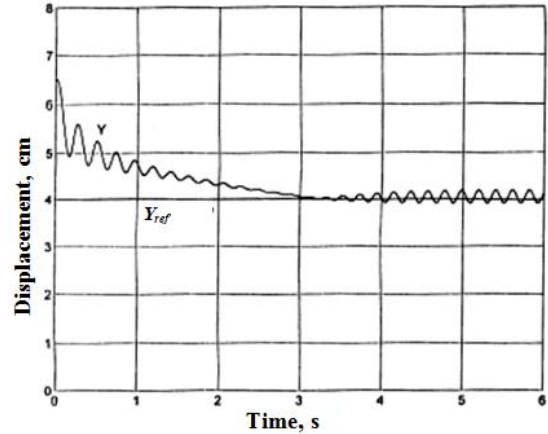
Fig.7 Control system response with CNNC set up for $e_{initial} = -2.5$ cm

7.2. Results of the PNNC

7.2.1. Single control point comparison with the CNNC

The PNNC showed a successful control results, as it is expected, for single control point in both movement directions. A single universal set up is needed to cover a wide range of control point conditions. While the CNNC set up for $e_{initial} = 4$ failed to cover $e_{initial} = 5.5$ cm as shown in figure 6, the PNNC successes to cover multi control conditions as figures 8 and 9, below, show.

7.2.2. Tracking control results for the PNNC

Figures 8 and 9 show tracking control results of PNNC for two different tracking trajectories. In both trajectories, reasonable settling time and steady state error are achieved. The figures also show that, in both of movement directions, the piston shows an oscillatory movement forward and backward on his way from its initial position to its reference position. This is because of the high nonlinearity behavior of the pneumatic systems.
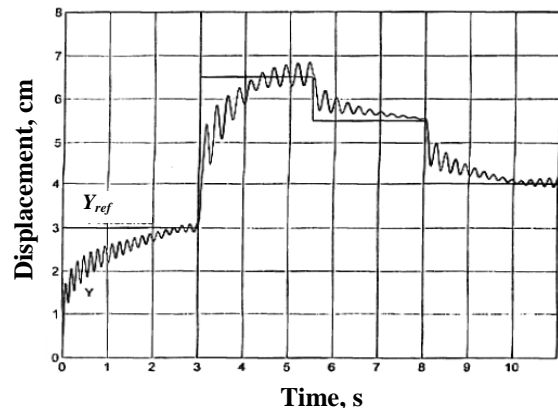
Fig.8 Tracking control results with PNNC, track trajectory 1
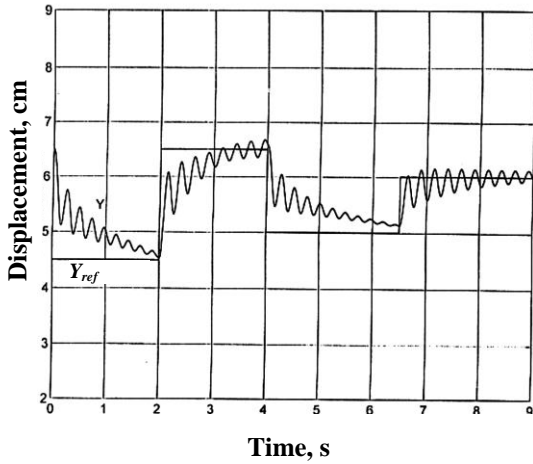
Fig.9 Tracking control results with PNNC, track trajectory 2

7.2.3Comparison with the results of the conventional PI controller

The conventional PI controller is tested as a position controller of the present pneumatic system.

Time, s
P   controller,   Kc

Time, s
PNN
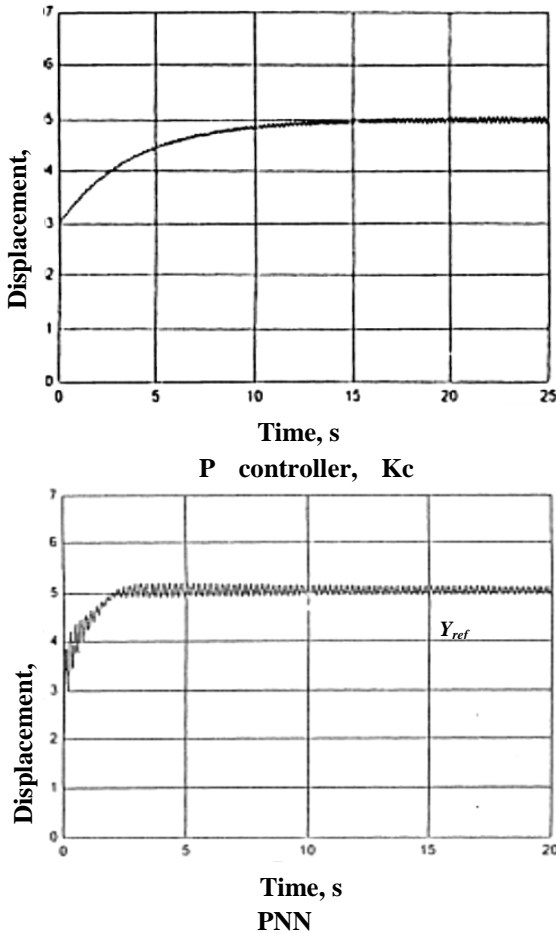
Fig.10 Comparison between control results for the PNNC and the P controller

The proportional gain, *Kc*, has to be very small to avoid system instability. This is because of the high nonlinearity of the controlled plant. The largest value of *Kc* was found

to be equal to 0.3, above which the control system becomes instable. Of course this leads to a large settling time. The integral effect was found to reduce the settling time but it increases the system instability, and thus it is excluded.

Figure 10 shows a typical comparison between control results of both the PNNC and the P controller of the largest possible gain, *Kc = 0.3*. The P controller shows stable results with large settling time, 15 seconds. The PNNC shows small settling time, 2 seconds, with relatively allowable oscillations which are slowly converged with time, as shown in the figure.

The conventional P controller does not give satisfactory results when applied to pneumatic systems. So, neural network controllers are proposed to do the job.

7.2.4Testing the PNNC against load disturbance

The load disturbance effect on the PNNC performance is shown in Figure 11. The load value changes in range of about ± 0.90% of a design load of 5.5 kg. The load disturbance is generated using a white noise generator built in facility of the MATLAB-SIMULINK commercial package. The figure shows the robustness of the PNNC to severe fluctuation in the applied load and still showing fairly good results.
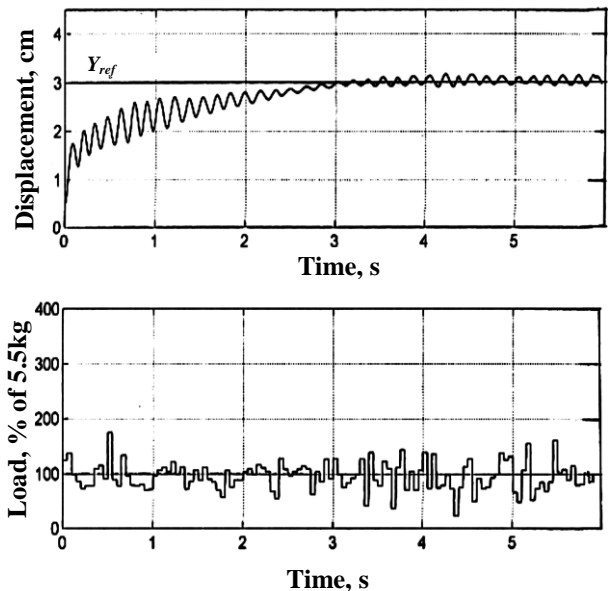
Fig.11 Effect of external disturbance ± 90% around a design load of 5.5 kg

Conclusions

A mathematical nonlinear model is derived for a double acting pneumatic cylinder plant. A rule based NN controller is proposed, PNNC, and applied to positional control the piston movement of the present pneumatic system. The robustness and effectiveness of the proposed controller were verified through computer simulations using MATLAB package and SIMULINK toolbox. The performance of the present PNNC was tested against the PI and the conventional NN controllers. The main conclusions are extracted as follows:

1) The conventional NN controller, CNNC, gives satisfactory control performance for a single control condition.
2) The proposed NN controller, PNNC, successfully achieves a good tracking control performance for a wide range of control point conditions.
3) The PNNC shows a satisfactory control performance for load disturbance of about ±70% of the load design value.

Appendix A

The pneumatic system initial conditions are set as follows:
Initial pressure: 3.5 bar
Air tank pressure: 2.94 bar
Supply air pressure: 6.0 bar
Supply air temperature: 298 K
Air inside cylinder initial temperature: 298 K
Air tank initial temperature: 298 K
External load: 5.5 kg
Cylinder diameter: 2.5 cm
Stem Diameter: 1.0 cm
Supply tube diameter: 1.0 cm
Discharge tube diameter: 1.0 cm
Piston stroke: 7.0 cm
Initial piston velocity: 0.0 m/s
Gas constant: 287 J/(kg K)
Specific heat ratio: 1.4

ANN Controller Parameters

The value of the ANN controller's parameters, $W_{initials}$, $\theta_{initials}$, $\delta_{initials}$, and $\eta_{initials}$ and the slope parameter β were obtained as explained in the paper and listed below for both the forward and backward piston's movement.

Forward Piston Movement

The selected parameters are determined at $\beta = 1$ and for $e_{initial} = 2.50$ cm, $y_{ref} = 3$ cm and $y_{initial} = 0.5$ cm were:
$W_{initials} = 10^{-6}$
$\theta_{initials} = 1 \times 10^{-3}$
$\delta_{initials} = 1 \times 10^{-3}$
$\eta_{initials} = 0.1$.

The slope parameter -initial error (β - $e_{initial}$) relation is obtained as $\beta = \sum_{i=0}^{6} a_i\, e_{initial}^{i}$

Where: $a_0 = 0.0021$, $a_1 = -0.0569$, $a_2 = 0.6238$, $a_3 = -3.5700$, $a_4 = -11.4616$, $a_5 = -20.0931$, $a_6 = 16.9828$.

Backward Piston Movement

The selected parameters are determined at $\beta = 1$ and for $e_{initial} = -3.50$ cm, $y_{ref} = 3$ cm and $y_{initial} = 6.5$ cm were as follows;
$W_{initials} = 10^{-6}$
$\theta_{initials} = 0.2$
$\delta_{initials} = 0.1$
$\eta_{initials} = 0.078$

The slope parameter -initial error (β - $e_{initial}$) relation is obtained as $\beta = \sum_{i=0}^{6} a_i\, e_{initial}^{i}$

Where: $a_0 = -0.1262$, $a_1 = -1.6587$, $a_2 = -8.6556$, $a_3 = 22.58$, $a_4 = -29.93$, $a_5 = 16.6413$, $a_6 = 0.83$

List of symbols

A	Cross-sectional area, m^2
Subscripts	
C	Cylinder inlet connection
pl	Piston left side
pr	Piston right side
S	Supply air connection
v_1	Valve1 orifice
v_2	Valve2 orifice
ANN	Artificial neural network
$ANNC$	Artificial neural network controller
BP	Back Propagation
C_{d1}	Coefficient of discharge, valve 1
C_{d2}	Coefficient of discharge, valve 2
C_p	Specific heat at constant pressure
F_c	Coefficient of viscous friction
CNN	Conventional Neural Network
$CNNC$	Conventional Neural Network Controller
e	Error signal $y_{ref} - y(t)$
m_1	Mass flow rate through valve1, kg/s
m_2	Mass flow rate through valve2, kg/s
M_l	External load, kg weight = $9.8\,N$
NN	Neural Network
U	Internal energy of system, J
O	Sum of node outputs = inputs to next layer nodes
P	Pressure, Pa/m^2
Subscripts	
a	Atmospheric
c	Cylinder at right side
l	Cylinder at left side, Tank side
R	Reduced pressure ratio through the valve
s	Supply air
$PNNC$	Proposed Neural Network Controller
PWM	Pulse width modulation
Q	Rate of heat transfer across the wall of cylinder, W
R	Gas constant, $J/(kg\ ^ok)$
t	Time, sec
T_a	Atmospheric Temperature, ^oK
T_c	Temperature of air inside the cylinder, ^oK
T_s	Temperature of supply air, ^oK
V_c	Volume of the right side of the cylinder
W	Weight of ANN node
X	Output of ANN node
y	Piston displacement, m
y_{ref}	Piston reference position, m
$y_{initial}$	Piston initial position, m
$\dot{y}$	Piston velocity, m/s
$\ddot{y}$	Piston acceleration, m/s^2

Greek letters

γ	Specific heat ratio
β	Slope parameter
ρ_c	Air density at right side of cylinder, kg/m^3
ρ_s	Supply air density, kg/m^3

ρ_{v1} Air density after valve 1, *kg/m^3*

ρ_{v2} Air density after valve 2, *kg/m^3*

Θ Bias of ANN

δ Learning rate of ANN

η Gain of ANN

References

N. Ishak, M. Tajjudin, H. Ismail, M. Hezri, Y. Sam, R. Adnan, (2012), PID Studies on Position Tracking Control of an Electro-Hydraulic Actuator, *International Journal of Control Science and Engineering, 2(5),pp.* 120-126.

Moore J. R., Wong C.B., (2000), Smart Components-based servo pneumatic actuation systems, *Microprocessors and Microsystems, Vol. 24,* pp. 113-119.

Tillet N.D., Vaughan N.D., Bowyer A., (1997), A Non-linear model of a Rotary Pneumatic Servo System, *Proc. Instn Mech Engrs, Vol. 211, Pert 1,* pp. 123-133.

Shih M.C., Ma M.A., (1998), Position Control of a Pneumatic Cylinder Using Fuzzy PWM Control Method, *Int. Journal of Mechatronics, Vol. 8*, pp. 241-253.

Varseveld R.B., Bone G. M., (1997), Accurate Position Control of a Pneumatic Actuator Using On-Off Solenoid Valves, *IEEE/ASME TRANS. On Mechatronics, Vol. 2 No. 3,* pp. 195-204.

Fujiwara, K. K., Ishida Y., (1995), Neural Network Based Adaptive I-PD Controller for Pneumatic Cylinder, *SICE, Sapporo*, pp. 1281-1284.

Cui, X., Shin, K.G., (1992), Application of Neural Networks to Temperature Control in Thermal Power Plants, *Eng. Appl. Artif. Intell., Vol. 5, No. 6,* pp. 527-538.

Abdelhameed, M.M., (1999), Adaptive Neural Network Based Controller For Robots, *International Journal of Mechatronics, Vol. 32, No.2,* pp. 211-224.

G. Geng, G. M. Geary, (1997), Application of a Neural-Network-Based RLS Algorithm in the Generalized Predictive Control of a Nonlinear Air-Handling Plant, *IEEE Trans. On Control Systems Technology, Vol. 5, No. 4,* pp. 439-445.

G. Cembrano, G. Welis, J. Surde, A. Ruggeri, (1997), Dynamic Control of a Robot Arm Using CMAC Neural Network , *Control Eng. Practice, Vol. 5, No. 4,* pp. 485-492.